sustainability

MDPI

Article

Confinement of Concrete Using Banana Geotextile-Reinforced Geopolymer Mortar

Vincent P. Pilien [1], Michael Angelo B. Promentilla [2], Julius L. Leaño, Jr. [3], Andres Winston C. Oreta [1] and Jason Maximino C. Ongpeng [1,*]

[1] Department of Civil Engineering, De La Salle University, Manila 0922, Philippines; vincent_pilien@dlsu.edu.ph (V.P.P.); andres.oreta@dlsu.edu.ph (A.W.C.O.)
[2] Waste and Resource Management Unit, Center for Engineering and Sustainable Development Research, De La Salle University, Manila 0922, Philippines; michael.promentilla@dlsu.edu.ph
[3] Research and Development Division, Department of Science and Technology, Philippine Textile Research Institute, Metro Manila 1863, Philippines; jlleanojr@ptri.dost.gov.ph
* Correspondence: jason.ongpeng@dlsu.edu.ph

Abstract: Geopolymer, a sustainable alternative to ordinary Portland cement (OPC), offers reduced embodied energy, lower carbon emissions, enhanced durability, eco-compatibility, and waste valorization potential. In confining structural members, geopolymer still has limitations with respect to its brittleness and other properties. Enhancing the properties of geopolymer by adding banana fibers (BF) and fly ash (FA) to form banana geotextile-reinforced geopolymer mortar (BGT-RGM) as confining material, is investigated in this experimental study. BGT-RGM is a textile-reinforced mortar with varying thickness of BF-reinforced geopolymer mortar (BFRGM) through NaOH-treated 10 mm BFs and 2 mm banana geotextile (BGT) having varied grid spacings. To develop BGT-RGM, the physical, mechanical, and chemical properties of the BFs were determined, while BFRGMs were evaluated for compressive and dog-bone tensile strengths, workability, scanning electron microscopy (SEM) imaging, and thermogravimetric analysis (TGA). The BGT-RGM-confined and unconfined concrete were evaluated, and the strength variations were imparted by the confinement as reflected on the stress-strain curves. The local crack formation mode of failure was also determined through crack patterns during an axial load test. The BGT-RGM with 20 mm thickness of BFRGM with 15 mm and 20 mm geotextile grid spacings, exhibited 33.3% and 33.1% increases in strength, respectively. Future investigations towards the development and application of BGT-RGM are also discussed.

Keywords: banana geotextiles; natural fiber; banana fiber; coal fly ash; textile-reinforced mortar; microstructure; green mortar

Citation: Pilien, V.P.; Promentilla, M.A.B.; Leaño, J.L., Jr.; Oreta, A.W.C.; Ongpeng, J.M.C. Confinement of Concrete Using Banana Geotextile-Reinforced Geopolymer Mortar. *Sustainability* **2023**, *15*, 6037. https://doi.org/10.3390/su15076037

Academic Editor: Jonathan Oti

Received: 11 February 2023
Revised: 18 March 2023
Accepted: 22 March 2023
Published: 30 March 2023

1. Introduction

Textile-reinforced mortar (TRM) has emerged as a practical and efficient technique for enhancing the performance of concrete structures. The confinement provided by TRM leads to significant improvement in the concrete's axial load capacity and overall durability [1]. However, traditional TRMs and fiber-reinforced cementitious matrices (FRCMs) are commonly made from ordinary Portland cement (OPC) matrices and synthetic fibers (SF). Indeed, Toska & Faleschini [2] studied FRCM using cement-based mortar reinforced with carbon and glass fibers in reinforcing reinforced concrete, and concluded that the right amount of FRCM confinement reduced the lateral expansion of concrete and improved the axial resistance of concrete. Likewise, Patel et. al. [3], explored the use of waste materials as replacement of cement in mortar mixtures aiming to lessen the significant negative impact of cement production that generates 5% of CO2 and 7% of industrial used fuels globally. In order to address the issues of: excessive CO2 emissions resulting from OPC production; the unavoidable cracks gained by concrete due to the tests of time, changes in weather and wrath of disasters; and the potential of fly ash

and BF waste valorizations, this paper presents the development of a banana geotextile-reinforced geopolymer mortar (BGT-RGM), a sustainable and eco-friendly alternative to conventional TRMs. The replacement of ordinary Portland cement (OPC) and synthetic fiber in BFRGM applications could yield several benefits. For example, these encompass a consequent decline in CO_2 emissions, and increased resilience of materials against aging, environmental factors, and extreme heat conditions. Furthermore, the assimilation of fly ash and banana fiber as a means to valorize both industrial and agricultural by-products, circumvents the reliance on industrially manufactured textile-reinforced mortars (TRMs) and OPC. Collectively, these advances highlight the promising potential of BFRGM within the fiber-reinforced geopolymer concrete research domain.

Geopolymer mortar is an alkali-activated material that has been gaining attention as a sustainable and green alternative to OPC mortar [4]. Unlike OPC mortar, geopolymer mortar requires minimal energy to process, resulting in a lower embodied carbon footprint, and it can be made from industrial waste materials like coal fly ash [5,6]. Thus, geopolymer-based materials have been considered a sustainable alternative to traditional cementitious building materials for decades, due to their constant design improvement and advancement [7]. However, geopolymers, like OPC mortars, are brittle and susceptible to cracks, which can lead to brittle failure [8]. This weakness can be mitigated by using fibers as reinforcement, which can provide crack bridging [9] and increase ductility [10].

To produce a more sustainable material, this study proposes the use of natural fibers (NF) such as BFs, as a replacement for SFs. Since the global need for innovative, environmentally friendly, and sustainable green textiles is quickly rising, many industries have adopted NFs which are abundant and renewable, like the BFs which are widely used in many fields [11]. In order to modify the physical and mechanical characteristics of BFs, a chemical treatment must be conducted. The use of alkali effectively renders natural textile fibers, especially lignocellulosic fibers, more processable from raw to textile form. The use of NaOH is common in textile processing, and its management allows community deployment to banana farming communities, with dilution and/or neutralization deployed as strategies for management after use. The further valorization of extractives through precipitation of e.g., lignin, using acids, technically manages the pH. As further stated by Camargo et al. [12] and performed by Pilien et al. [13], 4% of NaOH as alkaline treatment for banana fibers within 4 h shows significant increase in strength. In addition, the NaOH treatment of BGT significantly improved the mechanical, chemical, and physical properties of the fibers. The treated BFs (TBFs) had a tensile strength improvement of 83.60%, and roughened the surfaces of the fiber, which enhanced bonding between the fiber and the matrix, as shown in the SEM analysis. Debonding and cracks were also observed in the SEM analysis. Furthermore, Muthu et al. [14] revealed the negative environmental impacts of SFs on the environment, including its non-renewable source, higher energy requirement and greenhouse gas emissions during the production process, synthetic fiber (SFs) waste disposals due to non-biodegradability which may cause toxic pollution, and considerable volumes of chemicals used to manufacture these synthetic fibers. These shows the significant reductions on the environmental impact of using natural textile fibers (NTFs) over the synthetic fibers, with just a very small amount of NaOH used for treatment.

Alkaline treatment prevented the bond of hydrogen and removed impurities, hence elevating its mechanical and physical characteristics. In terms of the long-term effects of alkali treatment, it also reduced the fiber's hydrophilic characteristics [15], which can protect fibers from absorbing water and other substances that may cause decomposition of natural textile fibers like BF. Likewise, from the study of Sivaranjana and Arumugaprabu [16], the BF-reinforced polymer composite reveals that it has greater thermal stability than other natural fibers, which increases the numbers of its applications in industry as a temperature-resistant composite. It further elaborates that BFs give an excellent moisture resistance.

NFs are cheaper and are considered waste, making them abundant and locally available [17]. They are also renewable, biodegradable, and non-toxic [12]. Studies have been conducted on sisal and BF reinforced composites, proving the strength of BFs [18,19]. BFs

have reported high mechanical characteristics compared to other NFs, making them a viable reinforcing material for a wide range of engineering applications [19,20]. Moreover, hybrid short fibers have also been used for mortar reinforcement, and long fibers for textile reinforcement [21]. However, NFs are not included in the state-of-the-art review of TRMs by Koutas et al. [22] which focuses on synthetic fibers as textiles.

Utilizing banana short fibers as reinforcement in concrete and other cementitious composites has been proven to be an effective method to increase the compressive strength. According to the study of Anath et al. [23], incorporating 0.2% of banana fibers (BFs) into the concrete mixture resulted in a 19% increase in compressive strength. Ali et al. [24] also reported an 18.18% increase in compressive strength with 0.5% BF incorporation, while Bharathi et al. [18] observed a 51% increase in compressive strength with 1% BFs in the concrete mixture. Mostafa and Uddin [25] even recorded a remarkable increase of 77% in compressive strength and 94% in flexural strength when 1% of BFs was incorporated with Concrete Earth Blocks (CEB). These findings highlight the potential of banana fibers as a reinforcing material in concrete composites.

The types and design mixes of geopolymer which affect the composite's durability, that in turn influence the formation of cracks, were put forward in a previous study of Wyom Paul et al. [26]. In this study, the design of the experiment was adopted from the work of Pilien et al. [27], who performed an optimization on the fly ash-based banana fiber reinforced geopolymer mortar (BFRGM). Furthermore, based on the intensive review of Koustas et al. [22] on TRMs with synthetic fibers, the compatibility of BGTs with the BFRGM were also investigated.

This study thus aims to investigate the feasibility of utilizing BGT-RGM as a means of confining concrete. To the best of the researchers' knowledge, this application has not yet been thoroughly explored, making it an important area of research in the field of natural fiber-reinforced geopolymer composites. The BFRGM is composed of NaOH and sodium silicate (Na_2SiO_3) activator, blended with fly ash (FA), sand, and silica fumes (SiO_2). The reinforcement used in the BGT-RGM is comprised of hybrid short and long BFs, which serve as an environmentally sustainable alternative to synthetic fibers. Key parameters considered in this study include the thickness of the BFRGM and the spacing of the BGT grids. The thickness of the mortar was patterned on the study of Toska and Faleschini [2], using 5–20 mm thickness for cementitious based mortars. To ensure the full impregnation of the 2 mm thick BGTs, and considering its lap totally wrapped the concrete sample, producing two layers of BGTs on the lap zone, mortar thickness covering must be investigated, hence 12 mm and 20 mm of BGT-RGM were considered. Likewise, the grid spacing varies from 15 mm to 20 mm and 25 mm, to allow the short fiber reinforcement of the BFRGM to penetrate freely in any direction both before and after the BGTs application. In addition, the grid spacing is an important factor in the impregnation of textiles [22]. The methodology for preparing the BFRGM and the associated experimental program and testing procedure are described in detail in Section 2. In this section, the preparation of the BGTs and banana short fibers are presented. The results of the study are analyzed and discussed in Section 3, and finally, Section 4 concludes the study and outlines future work and directions, such as the potential inclusion of concrete healing agents on the mortar, which can reduce CO_2 emissions, enhance its mechanical properties, and repair the fracture from cracks caused, for example, by, hydration due to heat, change in volume, and change in the environment [28].

2. Materials and Methods

2.1. Materials

2.1.1. Banana Fiber Reinforced Geopolymer Mortar (BFRGM)

The banana fiber reinforced geopolymer mortar (BFRGM) in this study was prepared using coal fly ash (FA) as its geopolymer precursor and banana fiber as the reinforcing material. The FA was sourced from Pozzolanic Inc. Philippines, while the banana fibers (BFs) were from a local plantation in Vigan City.

Figure 1 shows the composition of BFRGM. Banana fibers (BF) from pseudo stems with 10 mm length were used as reinforcement of the BFRGM. The treatment process used 4% of NaOH mixed with 96% of water, to form the solution wherein a 1:30 liquor ratio was utilized [13]. This ratio was used to fully submerged all the BFs on the solution.

Figure 1. Banana Fiber Reinforced Geopolymer Mortar (BFRGM).

The geopolymer mortar was prepared by using FA and silica fumes (SiO_2) as binders and sand as filler, then it was activated by an alkali solution composed of NaOH and Na2SiO3. With the inclusion of SiO_2, which are commonly used pozzolanic material, in the geopolymer, the durability of the composite could be enhanced [29].

2.1.2. Banana Geotextile and Short Fiber Fabrication Process and Application

The BFs were extracted from the pseudo stem of the banana and treated with NaOH. The hybrid short and long fibers were fabricated after the curing period of the fiber treatment, as shown in Figure 2. The BGT fabrication process began with the twisting of BF strands to become a rope-like 2 mm yarn, by using an improvised twining machine stored in a cable, or yarn reels. The yarn was then woven into a wooden loom to form a banana geotextile. The spacing of the grids used were 15 mm, 20 mm, and 25 mm on both vertical and horizontal directions, and 5-strands of fibers to tie up the connections of fibers, as shown in Figure 3.

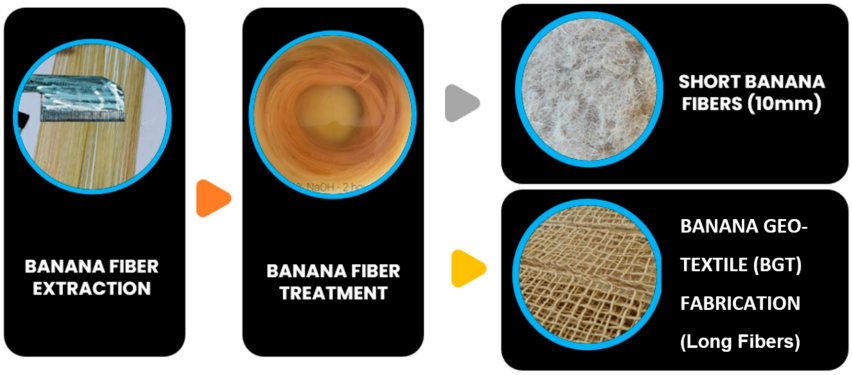

Figure 2. Banana Geotextile and 10 mm Short Banana Fiber Fabrication Flow Chart.

(**a**) (**b**) (**c**)

Figure 3. Banana geotextile fabrication: (**a**) improvised twining machine; (**b**) 2 mm BF yarn; (**c**) banana geotextile with 15 mm, 20 mm, and 25 mm grid spacings made from wooden loom.

Figure 3 shows the banana geotextile fabrication process, from twining BF strands to the production of yarns used in banana geotextile. The BGT is intended to reinforce the BFRGM by wrapping the first layer of BFRGM applied to the grade M15 concrete cylinder, followed by the final layer of mortar, to impregnate and fully cover the BGT. This is to enhance the axial load capacity of the M15 concrete through the BGT-RGM confinement.

The BF thickness and length-to-diameter ratios were not determined, since it was the fabricated hand twisted fibers that were used in the fabrication of geotextiles with greater than 2 mm yarn diameter from fabricated wooden looms. Future investigations will correlate these BF properties of thickness and aspect ratio to the processability into geoyarns, which are assembled into the desired specification of the geogrid.

2.1.3. Concrete Cylinder Samples

Note that the cylindrical concrete samples with M15 concrete mixture are expected to have a compressive strength of 15 MPa by the 28th day. Table 1 shows the specification of the materials used for the cylinder samples to be confined with BGT-RGM. These specifications were based on recent studies which investigated the strength variations of different confinement materials [30].

Table 1. Details of the concrete cylinder samples.

Materials	Specifications
Cement	OPC Type 1P
Fine Aggregates	Size < 9.5 mm
Coarse Aggregates	Size = 20 mm
Mixture	M15
Compressive Strength	15 MPa
Dimension	Diameter = 100 mm, Height = 200 mm

2.2. Methods, Design Mixtures and Experimental Designs

2.2.1. Design Mixture (DM)

Banana Fiber Reinforced Geopolymer Mortar (BFRGM)

Table 2 shows the design mixture of BFRGM, with the corresponding weights, in grams, of FA, SiO_2, sand, NaOH, WG, BFs, and waters, provided. Factors considered in creating the DM were: the water-to-solid ratio of 0.2; the NaOH-to-Na2SiO3 ratio of 0.54; the FA-and-SiO_2-to-sand ratio of 1.5; and the fact that 5% of SiO_2 and 1% of BFs were utilized. This DM is based on the studies of Quiatchon et al. [31] and Pilien et al. [27].

Table 2. BFRGM Design Mixture (DM).

	Sand (g)	(SiO_2) (g)	NaOH (g)	Water (g)	WG (g)	BF (g)	+Water (Kg) 10% FA	+Water (Kg) 200% BF	Molarity (M)
3600	2484	616	588	1285	1090	36	360	72	11.44

2.2.2. Banana Geotextile-Reinforced Geopolymer Mortar (BGT-RGM)

Banana Geotextile-Reinforced Geopolymer Mortar (BGT-RGM) Design of Experiment (DOE)

Table 3 shows: the 6 BGT-RGM designs and the control samples with 3 samples each; the thicknesses of the mortar, which are 12 mm and 20 mm; and the grid spacings, which range from 15, to 20, to 25 mm. The parameters of the banana geotextiles were based on recent studies. The grid spacings of some synthetic textiles range from 8 mm to 30 mm, with weights ranging from 150 g to 600 g per square meter, depending on the grid size [22]. The TRM shows great potential considering the downsides of fiber reinforced polymers, such as the compatibility of fiber to matrix and the crack proneness of geopolymer, similar to the studies of Cascardi et al. [32] on fiber reinforced mortar, Leone et al. [33] on glass fabric reinforced cementitious matrix, and Kariou et al. [34] on TRM.

Table 3. BGT-RGM Design of Experiment.

Specimen	Thickness of Mortar, mm	Grid Spacing, mm
BGT-RGM 1	12	15
BGT-RGM 2	12	20
BGT-RGM 3	12	25
BGT-RGM 4	20	15
BGT-RGM 5	20	20
BGT-RGM 6	20	25
CS	n/a	n/a

Banana Geotextile-Reinforced Geopolymer Mortar (BGT-RGM) Confinement Scheme

Figure 4 shows the 3 layers of the BGT-RGM, where the concrete cylinder diameter is 100 mm and coated with the 1st layer, making the diameter 114 mm, followed by the BGT and the 3rd and final layer, making the overall diameter 140 mm for the 20 mm thick BFRGM. For the 12 mm thick BFRGM, the 1st layer is 4 mm thick BFRGM, followed by the BGT and the 8 mm thick BFRGM final layer. The BGT grid spacings considered are 15 mm, 20 mm, and 25 mm, to allow the short BFs to penetrate in between the grids of the BGTs. A 10 mm allowance on both the top and the bottom of the cylinder was provided, to ensure that the confinement will not be damaged during the compressive test. This is to prevent direct compressive load and contact with the jacket [35].

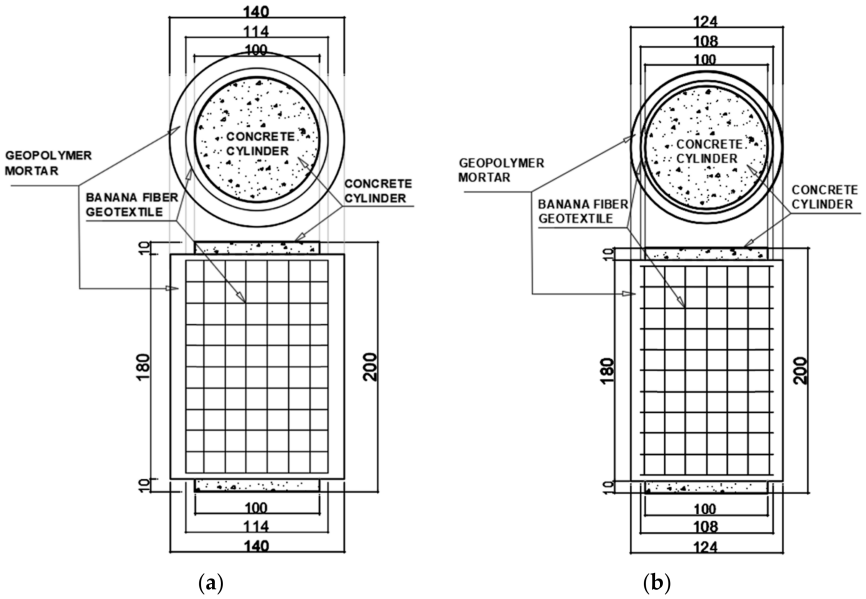

Figure 4. Banana Geotextile-Reinforced Geopolymer Mortar (BGT-RGM) Confinement Scheme: (**a**) scheme for 20 mm thick BGT-RGM, (**b**) scheme for 12 mm thick BGT-RGM.

Banana Geotextile-Reinforced Geopolymer Mortar (BGT-RGM) Confinement Procedures

Figure 5 shows the BGT-RGM concrete confinement process where the concrete cylinder's surface was roughened using sandpapers, and about 0.5 mm deep diagonal lines were grinded for the surface preparations. A PVC guide was used to mold the BFRGM with exact thickness both before and after the placing of the BGTs. Also, the PVC molds were used to ensure that there would be a 10 mm gap on both the top and the bottom of the concrete cylinder.

(**a**) (**b**) (**c**) (**d**) (**e**) (**f**)

Figure 5. Banana Geotextile-Reinforced Geopolymer Mortar (BGT-RGM) (**a**) concrete cylinder with roughened surface; (**b**) PVC molding guides; (**c**) application of the 1st layer of the BGT-RGM, (**d**) placing of the BGT as 2nd layer of BGT-RGM; (**e**) application of the final layer of the BGT-RGM; (**f**) plastic cling wrap on the BGT-RGM confined concrete.

After 24 h, the BGT-RGM confined concrete samples were wrapped with plastic cling wrap, both to ensure that alkali activators would not spill, and to avoid the occurrence of efflorescence that can significantly weaken the BGT-RGM [27].

2.3. BF, BFRGM and BGT-RGM Testing

2.3.1. Testing of Banana Fibers (BF)

Mechanical, physical, and chemical analysis of the treated and untreated banana fibers was conducted in order to investigate the effects of chemical treatment on BFs, and to ensure the quality of the fibers to be used.

Figure 6 shows the banana fiber testing equipment for the mechanical, physical, and chemical analysis, including the Instron-5966 UTM and ASTM1577-07 compliant fiber fineness apparatus. The Tenacity is derived from the tensile strength and the fineness of the fiber given by the following equation:

$$\text{Tenacity} = \frac{\text{cN (centiNewton)}}{\text{tex (fineness)}} \quad (1)$$

Equation (1) shows the tenacity of the banana fiber, which is equal to the peak load N multiplied by 100, divided by the fineness of the fibers.

(**a**) (**b**)

Figure 6. Testing of fibers: (**a**) tensile properties test, (**b**) fiber fineness test.

Laboratory wares such as glassware were also used, for the chemical analyses determining the moisture content, holocellulose, and lignin content, of the banana fibers.

2.3.2. Compressive Strength Test, Dog-Bone Tensile Test, and Flowability Test for BFRGM and Type S Mortar

Figure 7 shows the different tests conducted on the BFRGM to be compared with the Type S mortar, which is high strength mortar in terms of compressive strength and flowability. The dog-bone samples for the OPC mortar were damaged right after demolding the samples within 24 h. This is due to the absence of fiber to bridge the cracks caused by the brittleness of the OPC mortar.

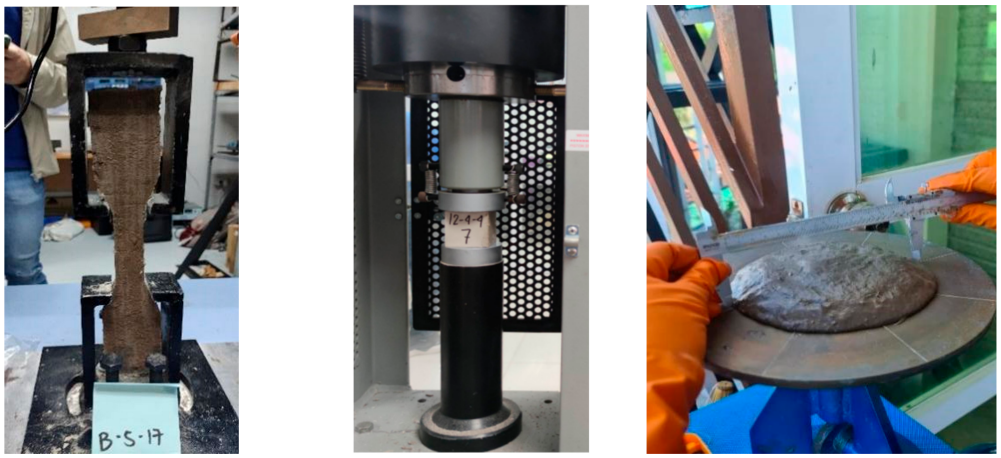

(**a**) (**b**) (**c**)

Figure 7. Testing of BFRGM: (**a**) dog-bone tensile test, (**b**) compressive strength test, (**c**) flowability test.

2.3.3. Thermal Gravimetric Analysis (TGA) for BFRGM and Type S Mortar

To determine the chemical phenomena happening during each process of degradation, a selected representative sample was tested from various types of materials. TGA was used to monitor sample mass with respect to temperature and time [36]. The Thermogravimetric—Differential Thermogravimetric (TG-DTG) and Differential Thermal Analysis (DTA) curves of the samples were provided from the analysis. The same parameters and treatment for OPC mortars were used when analyzing the BFRGM, wherein evident weight losses and corresponding peak temperatures in the TG-DTG curves and DTA peak temperatures were presented, to differentiate the traditional OPC mortar and the innovative BFRGM.

2.3.4. Scanning Electron Microscopy (SEM) Imaging for BFRGM and Type S Mortar

Scanning electron microscopy (SEM) imaging was performed for micrograph observation and elemental composition identification of fractured samples in order to characterize the BFRGM and to establish its properties and characteristics. From the study of Akinyemi and Dai [37], who performed SEM for the different composites, incorporating wood bottom ashes and banana fibers in the engineered cementitious composite (ECC) shows that the presence of cement hydrate products and fully bound polymer sheets, revealed the well-compacted interface in the composites. It was also determined that the BFs were fully coated by calcium silicate hydrates and polymer films that effectively bridge the gap between the fibers and the cement matrix.

In this study, the advantage of the elevated surface roughness of the BFs gained from chemical treatment were investigated and analyzed through scanning electron microscopy (SEM). The interaction of BFs and the geopolymer, voids, and other unusual observations, were also noted.

2.3.5. Testing for BGT-RGM Confined Concrete

Mechanical Strength Test of the BGT-RGM Confined Concrete

The BGT-RGM was tested using UTM to investigate the strength variations of the BGT-RGMs compared to the control samples.

Figure 8 shows the compressive strength test of the control samples and the BGT-RGM confined concrete samples after 28 days of curing using UTM. The BGT-RGM confined concrete and the control samples were compared in terms of compressive strength, to identify the strength variations provided by the BGT-RGM jacket.

(**a**) (**b**) (**c**)

Figure 8. Testing of BGT-RGM confined concrete: (**a**) BGT-RGM confined concrete samples, (**b**) control sample compressive strength test, (**c**) BGT-RGM confined concrete compressive strength test.

Crack Behavior and Mode of Failure

To study the crack behavior of the BGT-RGM confined concrete cylinders with different parameters, different configurations of textiles and different thicknesses of mortar coverings were used. The entire testing process was documented through capturing images every 10 to 15 s during the entire duration of specimen testing. The purpose was to monitor and maximize the investigation of crack propagation of specimens, and to identify the mode of failure of the samples, with the comparison of a BGT-RGM confined sample and the control sample.

3. Results and Discussions

3.1. Banana Fiber (BF) Test Results of Treated and Untreated Fibers

3.1.1. Mechanical and Chemical Analysis

The Mechanical analysis was carried out after the banana fiber treatment, using an Instron Universal Testing Machine (UTM). The mechanical analysis includes the tensile properties of fibers, the average breaking load (in newtons), and the average extension (in millimeters). The fineness of the banana fiber is also determined, through a fineness apparatus complying with ASTM 1577-07, and tenacity is assessed based on the tensile properties and fineness of the fibers.

3.1.2. Tensile Properties

Table 4 shows the results of the tensile strength test of banana fibers. The stronger fiber is the TBF with 4% of NaOH and 4 h of treatment, with a 3.36 N breaking load and 0.54 mm maximum extension. TBF has a tensile strength improvement up to 83.60% when compared to the untreated banana fiber (UBF). This result agrees with the image captured by optical microscope for TBF, which became rougher after treatment and signified the significant enhancement of fiber tensile properties when treated with NaOH, as shown in Figure 9.

Table 4. Average Breaking Load and Average Maximum Extension of Banana Fibers.

Sample	BF Treatment NaOH (%)	BF Treatment Time (Hrs)	Ave. Breaking Load (N)	Ave. Max Extension (mm)
Untreated-BF	0	0	1.83	0.56
Treated-BF	4	4	3.36	0.54

(**a**) (**b**)

Figure 9. Optical microscope images: (**a**) UBF; (**b**) TBF.

3.1.3. Chemical Analysis

Chemical analysis was undertaken in order to determine the holocellulose content of the banana fiber. Holocellulose is the water insoluble carbohydrate fraction of material from plants [38], while lignin is one of nature's most prevalent aromatic biopolymers, accounting for about 30% of all plants [39]. Treated banana fiber (TBF) has a lower lignin content, higher moisture content, and higher holocellulose, compared to untreated banana fiber (UBF). TBF has attractive chemical properties, higher performance when it comes to mechanical strength, and has a rougher surface, as captured by the optical microscope, which is also reflected in the value of its tenacity.

Table 5 shows the modifications provided by the chemical treatment, which reflects the 3.09% increase in moisture content, the 16.19% increase in holocellulose (cellulose and hemicellulose), and the 3.76% decrease in lignin content provided by the treatment. According to the study of Mahir et al. [40], the hemicellulose is responsible for the organic substance's decomposition, absorptions of moistures, and thermal decay of fibers, while lignin oversees UV-degradation. That study further stated that NFs generally contain 60 to 80% cellulose, 5 to 20% lignin, and up to 20% moisture content. From the results given in Table 5, the TBF and UBF are within these ranges, while the TBFs generally modified and performed better than the UBF, both mechanically and chemically.

Table 5. Moisture content, holocellulose, and lignin of banana fibers.

Sample	BF Treatment NaOH (%)	BF Treatment Time (Hrs)	Moisture (%)	Holocellulose (%)	Lignin (%)
UBF	0	0	9.54	63.94	13.38
TBF	4	4	12.63	80.13	9.62

3.1.4. Optical Microscope Imaging

The initial assessment of the treated banana fibers was conducted using an optical microscope, which allowed for a high-resolution image to be produced, with a magnification factor of 50 times, as depicted in Figure 9.

Figure 9 shows the magnified images taken by optical microscope for the NaOH treated banana fibers (TBF) and the untreated banana fibers (UBF). These images display

the modification of the surfaces of TBF which became rougher (b) compared to the UBF (a). These rough surfaces can interlock the bond between the fiber and the matrix, according to Camargo et al. [12]. The fibers that were soaked for 4 h in a 4% NaOH and 96% water solution, has darker color compared to the untreated banana fiber. This is due to the elimination of all impurities and lignin content, which made the fiber thinner and darker.

3.1.5. Physical Analysis, Average Fineness and Tenacity of Banana Fibers

The average fineness is expressed in terms of tex (grams per 1000 m of yarn), and tenacity is expressed in terms of cN/tex (centi-newton per tex). Fineness is tested using a fiber fineness apparatus, while tenacity is based on the average breaking load over average fineness of the fiber.

Table 6 shows the chemical analysis results of the treated and untreated banana fibers. The BF fineness refers to the number of fibers present in the cross-section of a yarn of a specific thickness that was used during the testing, while tenacity refers to the ability of a fiber to resist pulling or loading. The TBF has higher fineness, with 4.08 tex. This is due to the reduced thickness of the fibers which were removed during the chemical treatment. Likewise, the TBF has a tenacity of 94.9 cN/tex, which improves up to 7.4% when treated with NaOH. These results show the enhancement of fiber properties when treated with NaOH.

Table 6. Average fineness and tenacity of banana fibers.

Sample	BF Treatment NaOH (%)	BF Treatment Time (Hrs)	Ave. Fineness (tex)	Tenacity (cN/tex)
UBF	0	0	2.21	88.36
TBF	4	4	4.08	94.9

3.2. Banana Fiber Reinforced Geopolymer Mortar (BFRGM) Test Results

3.2.1. Mechanical Strength

Banana Fiber Reinforced Geopolymer Mortar and Type S OPC Mortar Compressive Strength Test Results

Table 7 shows the compressive strength, flowability, and spread diameter of the BFRGM and Type S OPC mortar.

Table 7. Compressive strength, flowability and spread diameter of BFRGM and OPC mortar.

Sample	Days	Flowability, %	Spread Diameter, cm	Compressive Strength, MPa
OPC Mortar	28	83.50	14.08	15.17
BFRGM	28	64.33	13.98	24.57

Type S OPC mortar has high strength with strong bond, based on ASTM C270 with 12.40 MPa compressive strength. Hence, the Type S mortar in this study exhibits 15.17 Mpa after 28 days, which is higher than the specification of ASTM C270. But the BFRGM is still 62% higher in terms of compressive strength, compared to the Type S OPC mortar. It was also observed during the test that the flowability values and the spread diameter of the OPC mortar is greater than the BFRGM. This is due to the presence of banana fibers on the BFRGM, which made it more compact, similar to the studies of Anath et al. [23], and Ali et al. [24], that showed significant increase in strength when incorporating short BFs.

Dog-Bone Test

The dog-bone test was conducted using a universal testing machine to determine the tensile strength of the samples. The dog-bone samples were casted with 13 mm thickness, with overall length of 330 mm, width of 60 mm, and with 30 mm necking, as shown in Figure 10. The slenderness of the samples made the samples prone to cracks, especially in

the case of OPC Mortar, where cracks occurred on the neck of the dog-bone samples even before demolding the specimen for curing. The BFRGM dog-bone samples also possessed micro cracks, but, due to the presence of banana fibers, the samples were demolded without breaking and were thus able to be tested after the curing period. The dog-bone tensile strength reached 0.79 MPa only, as shown in the stress and strain diagram of the sample shown in Figure 11. The thickness of the dog-bone samples is responsible for this result, and therefore an increase in the thickness of the dog-bone samples, in order to avoid early cracking and to have a successful comparison of BFRGM and OPC mortar, is highly recommended.

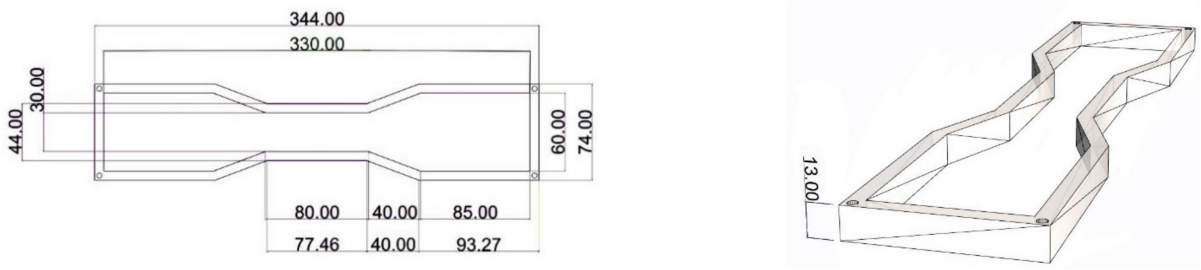

Figure 10. Dog-bone mold.

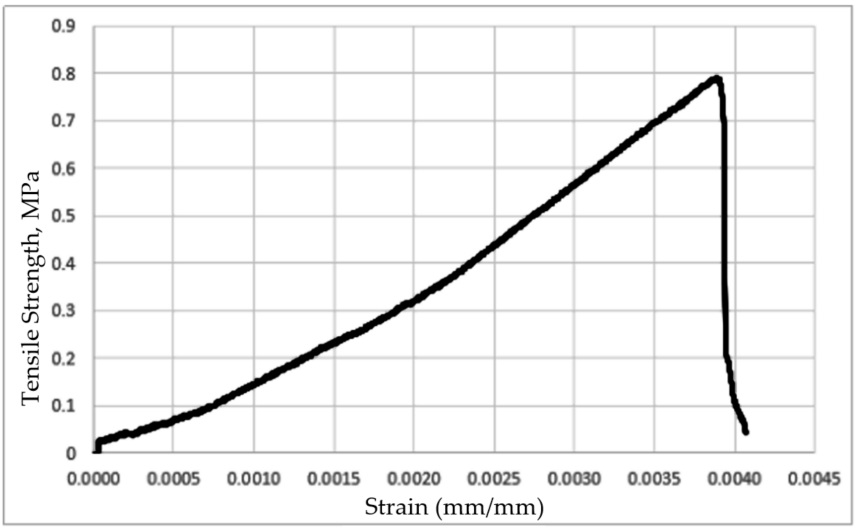

Figure 11. BFRGM dog-bone stress and strain diagram.

Figure 10 shows the dog-bone mold plan and the 3D perspective used to mold the slender samples that caused early cracking and low tensile strength of the specimens.

Figure 11 shows the stress and strain diagram of the dog-bone specimen tested for tensile strength. The tensile strength reached up to 0.79 MPa, and reached up to 0.00389 mm/mm strain. The stress and strain values were recorded using a universal testing machine and LVDT connected to the sample.

3.2.2. Microstructural Analysis

Thermal Gravimetric Analysis (TGA) for BFRGM and Type S Mortar

The thermogravimetric analysis (TG) and differential thermal analysis (DTA) curves of the Type-S OPC mortar are presented in Figure 12. The weight loss and derivative weight loss of the samples was tabulated in Table 8, which showed a significant loss of 2.876% of the original weight between 30 and 210.62 °C, with a peak temperature of 72.30 °C. The maximum weight loss of 11.316% was observed between 636.39 and 794.72 °C, with a peak temperature of 746.80 °C. At the end of the analysis, 85.808% of the weight of the Type-S mortar sample remained as residue. The DTA peaks at 85.82 and 750.04 °C correspond to

the weight loss, indicating endothermic processes due to the evaporation of free water and bonded water, which absorbed a significant amount of heat.

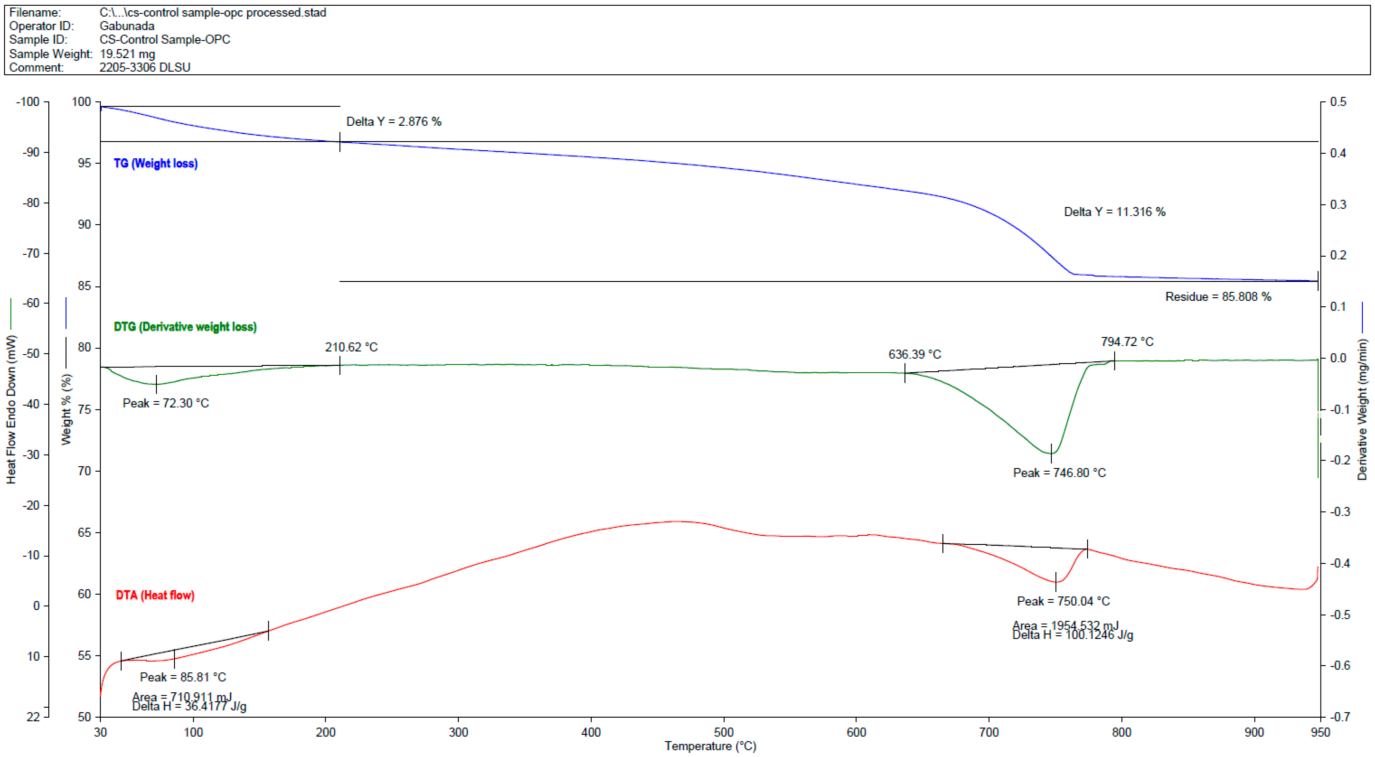

Figure 12. Differential Thermogravimetric (TG-DTG) and Differential Thermal Analysis (DTA) curves of the Type-S OPC Mortar.

Table 8. Thermal Gravimetric Analysis (TGA) for BFRGM and Type S Mortar.

Sample ID	Weight, mg	Weight Loss, % with Corresponding Peak Temperature	Peak Temperature (Tp), °C	Temperature Range, °C	Endothermic Peak Temperature (Tp), °C
Type S OPC Mortar	19.521	Weight loss 1 = 2.876 Weight loss 2 = 11.316 Residue = 85.808 Total = 100.000	Tp1 = 72.30 Tp2= 746.80	30.00–210.62 636.39–794.72	Tp1 = 85.81 Tp2 = 750.04
BFRGM	19.535	Weight loss 1 = 15.550 Residue = 84.450 Total = 100.000	Tp1 = 74.22	30.00–241.67	Tp1 = 82.57

The thermal analysis of the Banana Fiber Reinforced Geopolymer Mortar (BFRGM) was also analyzed through TG-DTA-DTA curves, as presented in Figure 13. The results showed a maximum weight loss of 15.550% of the sample's weight at a peak temperature of 74.22 °C, with 84.450% of the original weight of the BFRGM sample remaining as residue. The endothermic behavior of the sample was revealed through the DTA peak temperature at 82.57 °C, which was due to the evaporation of free and bonded water, requiring the absorption of a significant amount of heat. The accumulation of extra moisture and cracks could cause pore pressure, leading to spalling, especially if the pressure applied exceeds the resistance of the geopolymer [41]. This highlights the relationship between the water content and permeability of geopolymer mortars. As per the study of Zhang et al. [41], samples with high moisture content and low permeability tend to have more cracks and greater strength losses in geopolymer after exposure to high temperatures.

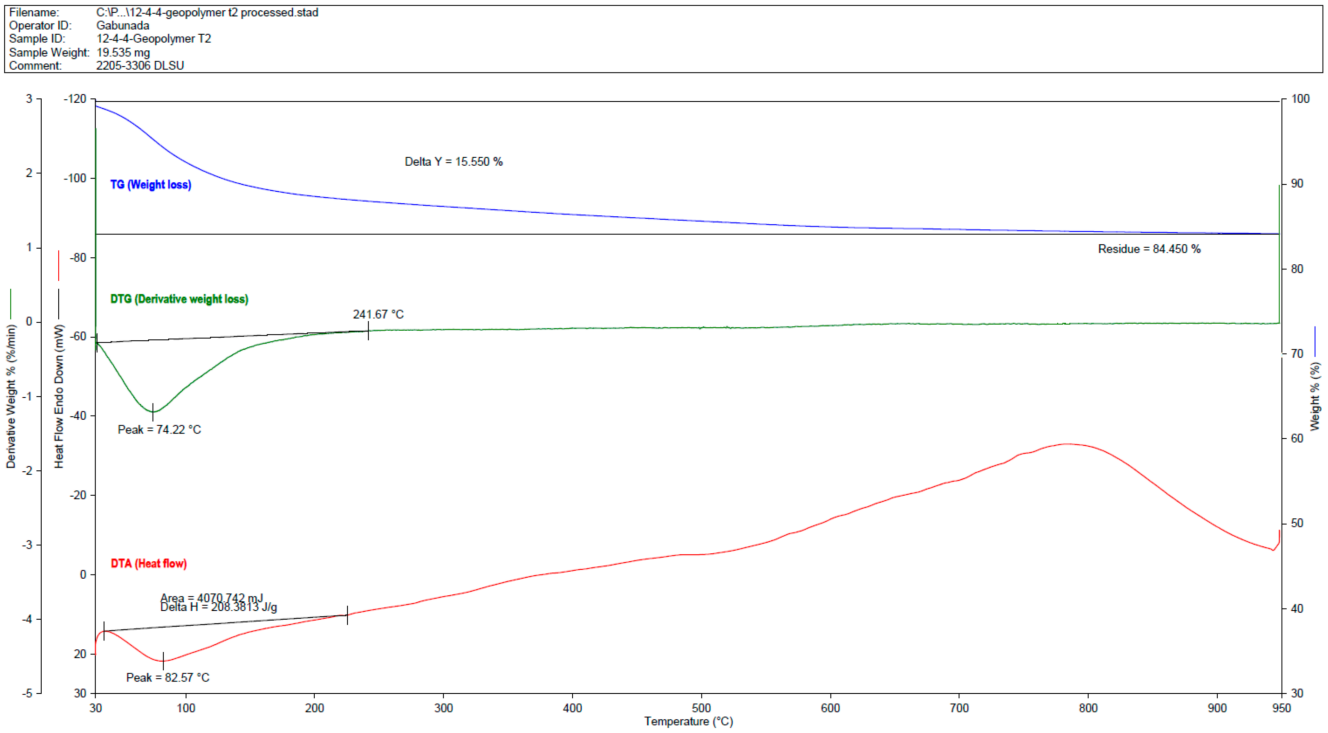

Figure 13. Differential Thermogravimetric (TG-DTG) and Differential Thermal Analysis (DTA) curves of the BFRGM Type−S OPC Mortar.

Scanning Electron Microscopy (SEM) for BFRGM and Type S Mortar

Scanning Electron Microscopy (SEM) for BFRGM

This study utilized the Thermo Scientific Phenom XL Scanning Electron Microscope (SEM) to analyze the microstructure of the samples. The SEM is equipped with a spacious chamber that can accommodate large samples, up to 100 mm × 100 mm in size. The following images were captured using the SEM during the analysis.

The images in Figure 14 are of the BFRGM sample that has the highest average compressive strength of 25.46 MPa. The banana fibers used in this sample were treated with 4% NaOH by mass for 4 h, which resulted in an enhanced appearance and roughness of the fiber, creating a better fiber-matrix interlock. The addition of banana fibers to the BFRGM matrix could improve strength, reduce cracks and shear stresses, and improve the bond between the fiber and the matrix [42]. The extent of cracks in the composite depends on various factors, such as the bond between the textile and the mortar, the strength of the fibers, and the quality of the textiles used, as noted by De Felice et al. [43]. SEM images captured in this study revealed pores and cracks in the matrix, debonding of fibers and matrix, rough surfaces between the geopolymer mortar and fiber, and some SiO_2 particles. These observations are consistent with previous studies, such as those conducted by Camargo et al. [12] and Naghizadeh et al. [44], which have shown that a modified abaca fiber with a rougher surface and uniformity can lead to improved compressive and flexural strength of the matrix. The findings of Riahi et al. [45] and Snellings et al. [46], on debonding and SiO_2 particles, respectively, were also confirmed in this study.

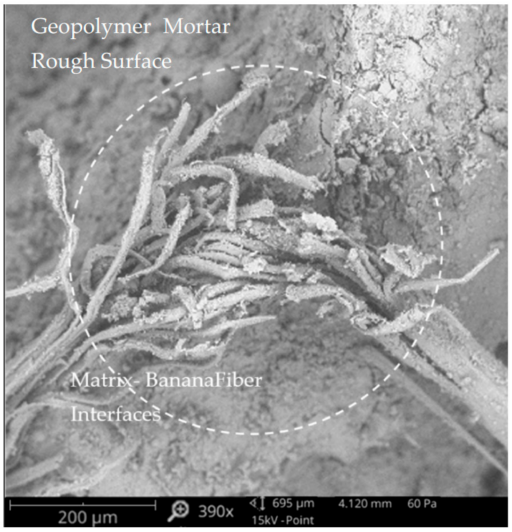

(**a**)

(**b**)

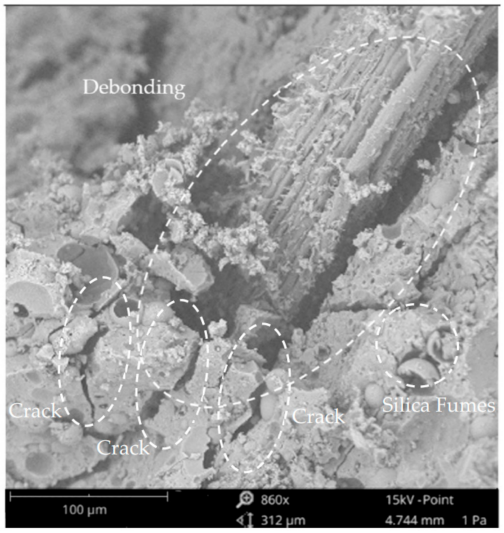

(**c**)

Figure 14. Scanning Electron Microscopy (SEM) for BFRGM: (**a**) BF and BFRGM matrix interface, (**b**) Banana fiber fully coated with BFRGM matrix, (**c**) BFRGM debonding.

Scanning Electron Microscopy (SEM) for Type-S OPC Mortar

As can be seen in Figure 15, the Scanning Electron Microscopy (SEM) for Type-S OPC Mortar shows the microstructures of the OPC mortar which contained micro-pores and gaps. Calcium hydroxide needles, which are one of the components of cement, were also observed on the images. The formation of some micro cracks are also visible within the OPC mortars.

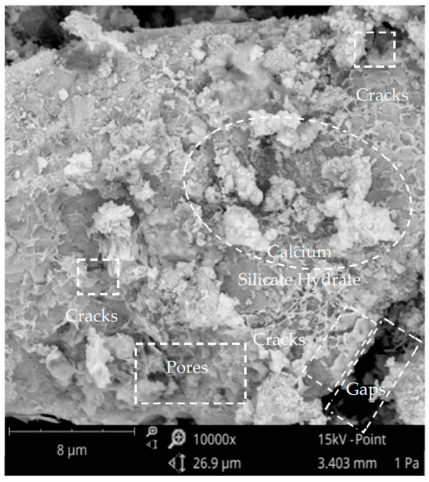

(**a**)

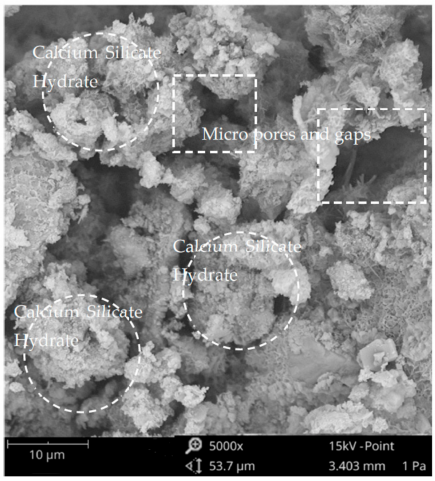

(**b**)

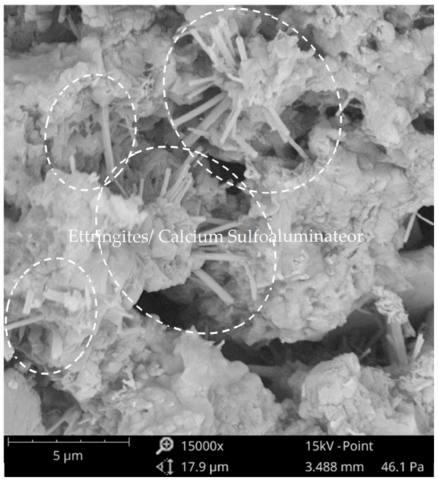

(**c**)

Figure 15. Scanning Electron Microscopy (SEM) for Type S OPC mortar: (**a**) 8 µm OPC mortar SEM image, (**b**) 10 µm OPC mortar SEM image, (**c**) 5 µm OPC mortar SEM image.

When it comes to an ordinary Portland cement mortar, the calcium sulfoaluminateor, the primary content of hydration on OPC, and calcium hydroxide and calcium silicate hydrate (CSH) gels, increased as it aged, and the microstructures and textures of the OPC mortar was elevated and became more complex within 28 days of curing [46,47].

3.3. Compressive Strength and Mode of Failure

3.3.1. Compressive Strength of BGT-RGM and CS

The compressive strength results of the BGT-RGM and control samples are presented in Figure 15, along with their respective standard deviations.

In Figure 16, it was observed that the use of 20 mm thick mortar provided higher compressive strength values compared to the 12 mm thick mortar, which gave lower axial load resistance provided by the BGT-RGM confinement. It was observed that the use of 15 mm and 20 mm BGT grid spacings provided higher compressive strength values, compared to the 25 mm BGT grid spacing. This is due to the huge gap in spacing provided by the 25 mm grid spacing, while the 15 mm and 20 mm BGT grid spacings are just enough to bond the 2 layers of BFRGM which impregnate the BGTs. The BGT-RGM 4 with 20 mm thick mortar and with 15 mm grid spacing, gave a 21.49 MPa of compressive strength, followed by BGT-RGM 5 with 20 mm thick mortar and 20 mm BGT grid spacing, which gave a 21.45 MPa compressive strength. Likewise, the standard deviation values of BGT-RGM 4 and 5 are 1.16 and 2.86, respectively.

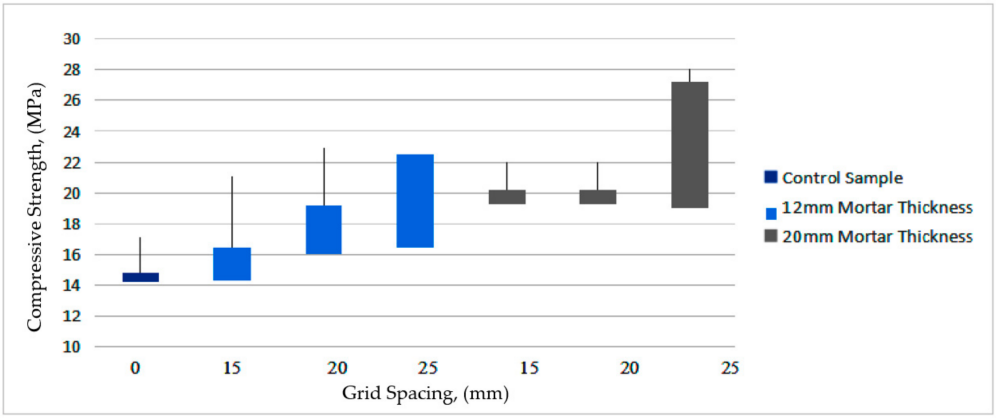

Figure 16. Compressive strength in relation to the thickness of mortar and rid spacing.

Figure 17 showcases percent increase in compressive strength and the standard deviations of the BGT-RGMs. The BGT-RGM 4 with the highest compressive strength provided an increase of 33.32% when M15 concrete was confined, followed by BGT-RGM 5 and 6, with increases of 33.08% and 29.50%, respectively. The results from BGT-RGM 1 to 3 with 12 mm thick mortar and varying grid spacings of BGTs from 15 mm to 20 mm, to 25 mm, provided a low compressive strength value from 17.28 MPa, to 19.38 MPa, and 17.08, respectively.

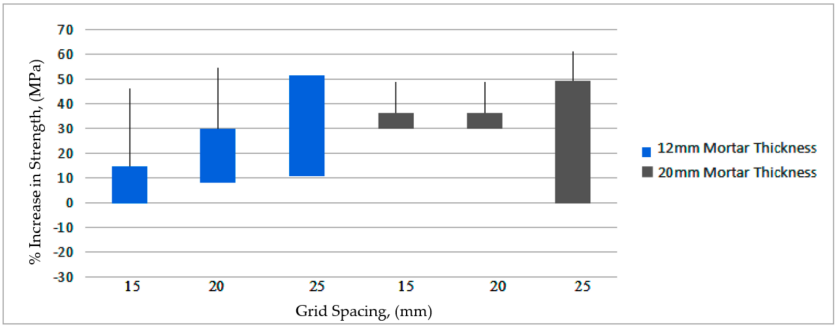

Figure 17. % increase in compressive strength provided by BGT−RGM compared to control sample.

These results from Figures 15 and 16 highlight that the BGT-RGMs with 20 mm thick mortar have higher compressive strength values compared to the BGT-RGMs with 12 mm thick mortar, while 15 mm and 20 mm grid spacing of BGTs gave higher compressive strength that 25 mm grid spacing of BGTs. This is due to the 15 mm and 20 mm yarn spacings allowing the short BFs to penetrate between the BGTs grid spaces. The 20 mm thick BFRGM reveals greater compressive strength, through the application of BFRGM layers in between BGTs that impregnate and bind the matrix.

Figure 18 is the Stress and Strain Diagram of the BGT-RGM 4 (1–3), which has compressive strength values of 22.03 MPa, 19.22 MPa, and 20.21 MPa. The BGT-RGM 4 samples were observed to have the same mode of failure caused by the rupture on the BGT-RGM jacket or confinement, and almost identical SSD curves. The ruptures of the jackets are shown in the Figure 18.

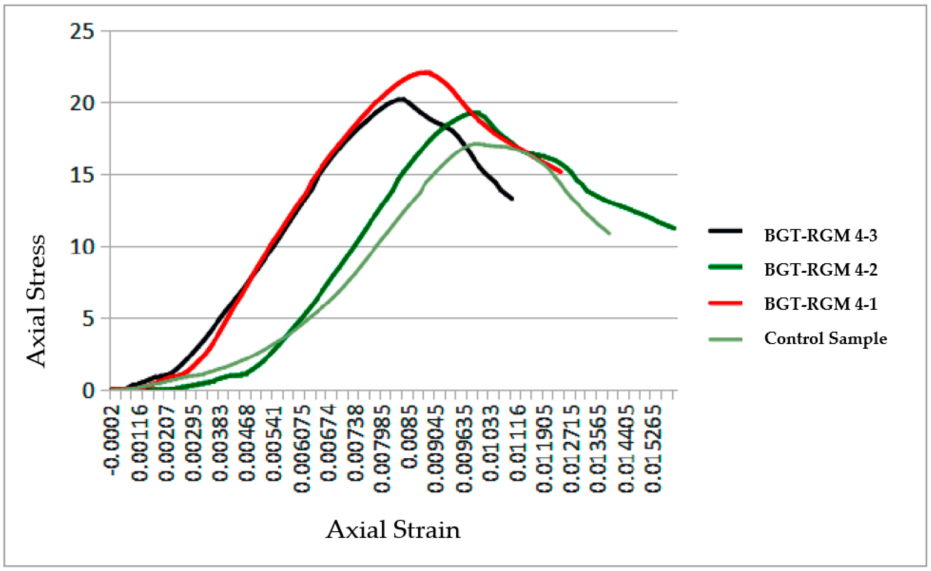

Figure 18. Stress and Strain Diagram (SSD) of BGT-RGM 4.

3.3.2. Mode of Failure of BGT-RGM and Control Sample

Figure 19 illustrates the cracked samples after the compression test using a universal testing machine. Figure 19a depicts cracks induced by unconfined concrete samples after the compression test, and Figure 19b depicts cracks initiated at the BGT-RGM confinement until it fails.

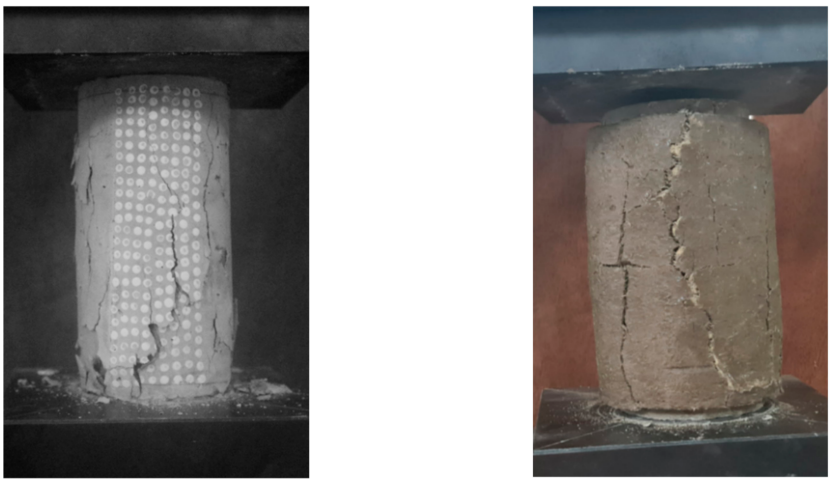

(**a**) (**b**)

Figure 19. Cracked sample specimens: (**a**) control samples, (**b**) BGT-RGM confined concrete.

The crack propagation was analyzed using digital images which were taken at 10 to 15 min intervals during the entire sample testing process. This was intended to maximize the observation of the crack initiations and mode of failure as shown in Table 9.

Table 9. Crack initiation and mode of failure of BGT-RGM and CS.

Sample	Crack Initiation	Mode of Failure
BGT-RGM 1	near mid-height	rupture of the jacket
BGT-RGM 2	near bottom	rupture of the jacket
BGT-RGM 3	mid-height	rupture of the jacket
BGT-RGM 4	mid-height	rupture of the jacket
BGT-RGM 5	mid-height	rupture of the jacket
BGT-RGM 6	mid-height	rupture of the jacket
CS	near bottom	shear and partial shear

Figure 9 shows the crack initiation and the mode of failure types. For the control samples (CS) or the unconfined samples, damages initiated through the formation of cracks near mid-bottom and mid-height of the samples. These cracks continued to form a longitudinal crack along the length of the cylinder. The cracks were extended to the upper and lower areas of the sample until it failed. For the majority of the BGT-RGM confined concrete, cracks initiated at the mid-height or near the top and bottom of the samples, which caused rupture on the BGT-RGM, which caused failure.

4. Conclusions and Recommendation

This study evaluates the potential of a banana geotextile-reinforced geopolymer mortar (BGT-RGM) confinement, through the analysis of the chemical, mechanical, physical, and microstructural properties of the material. The findings and conclusions are summarized as follows:

- The BFRGM had a compressive strength of 25.46 MPa, which was 62% higher than Type-S OPC mortar; had a 22.95% lower flowability percentage; and had a 0.71% lower in spread diameter that fully coated and impregnated the BGTs, resulting in the significant increase in strength provided by the BGT-RGM confinement, which exhibited up to 33.3% and 33.1% increases in strength from 15 mm and 20 mm BGT grid spacing, when each is coated with 20 mm BFRGM.
- The BGT-RGM compressive strength results indicated that the 20 mm thick mortar had better compressive strength compared to a 12 mm thick mortar, and accounted for the proper impregnation of the 15 mm and 20 mm geotextile grid spacing that allowed 10 mm short BGTs to penetrate along the geotextiles in all directions, which provided higher compressive strength values.
- The NaOH treatment of BFs significantly improved the mechanical, chemical, and physical properties of the fibers. The treated BFs (TBFs) had a tensile strength improvement of 83.60%, and the roughened surfaces of the fiber were found to enhance bonding between the fiber and the matrix, as shown in the SEM analysis. Debonding and cracks were also observed in the SEM analysis.
- The crack behavior of unconfined concrete had shear and partial shear failures, initiated near the mid-bottom and mid-height of the samples. The BGT-RGM confined concrete initiated ruptures from the jacket and continued along its length.
- High temperature resistance of BFRGM was shown in the TGA and DTG results, providing maximum weight loss of 15.55% of the sample's weight from a peak temperature of 74.22 °C, with 84.45% of the BFRGM left as residue. This shows that BFRGM composites exposed to high temperatures will only suffer weight loss on the peak load, with about 15.55% loss in the composite's weight.

This study thus recommends further exploration on potential applications of BGT-RGM technology, such as retrofitting of unreinforced masonry walls, arches, lintels, and eaves. This has the potential to reduce environmental impacts and minimize waste gener-

ated by power plants and large banana plantations. Another avenue of research could be to investigate the life-cycle impact of the process and product, including the scalability of BFRGM production, making it more accessible and economically viable for widespread use. Future work could also be done to further optimize the mechanical properties of BFRGM, such as tensile strength and ductility, making it a more competitive alternative to traditional materials. Correlation of the BGT properties such as thickness and aspect ratio to the processability into geoyarns which are assembled into the desired specification of the geogrid, is also of interest. In-depth analysis of the performance mechanisms of banana fiber-reinforced geopolymer mortars, such as the bonding effects of BFRGM and concrete, should be studied further. Likewise, the inclusion of a concrete self-healing agent on the mortar might give a significant boost to the concrete strengthening capability of the BFRGM. Finally, investigating the long-term durability and performance of BFRGMs in real-world applications would provide valuable insights for their practical usage.

Author Contributions: Conceptualization, V.P.P. and J.M.C.O.; methodology, V.P.P., M.A.B.P. and J.M.C.O.; formal analysis, V.P.P. and J.M.C.O.; investigation, V.P.P. and J.M.C.O.; resources, V.P.P., M.A.B.P., J.L.L.J., A.W.C.O., J.L.L.J. and J.M.C.O.; data curation, V.P.P., M.A.B.P. and J.M.C.O.; writing—original draft preparation, V.P.P.; writing—review and editing, V.P.P., M.A.B.P., A.W.C.O., J.L.L.J. and J.M.C.O.; visualization, V.P.P. and J.M.C.O.; supervision, M.A.B.P., A.W.C.O., J.L.L.J. and J.M.C.O. All authors have read and agreed to the published version of the manuscript.

Funding: This research received no external funding.

Institutional Review Board Statement: Not applicable.

Informed Consent Statement: Not applicable.

Data Availability Statement: Not applicable.

Acknowledgments: The Author would like to acknowledge the De La Salle University (DLSU), Materials for Sustainable Construction and Recyclables Applied to Projects (MSCRAP), Department of Science and Technology-Philippine Textile Research Institute (DOST-PTRI), the Joint Research Undertaking (JRU) between DLSU and DOST-PTRI for supporting this research, Bureau of Research and Standards (BRS), University of Northern Philippines (UNP) and Department of Public Works, Highways Region-I, and University of the Cordilleras and VPP staff, for their support and trust towards the success of this research.

Conflicts of Interest: The authors declare no conflict of interest.

References

1. Pilien, V.P.; Garciano, L.E.; Promentilla, M.A.; Guades, E.; Leaño, J., Jr.; Oreta, A.W.; Ongpeng, J.M. Banana fiber-reinforced geopolymer based textile reinforced mortar. In Engineering Proceedings, Proceedings of the 1st International Online Conference on Infrastructures, 7–9 June 2022; MDPI: Basel, Switzerland, 2022; Volume 17.
2. Toska, K.; Faleschini, F. FRCM-confined concrete: Monotonic vs. Cyclic axial loading. *Compos. Struct.* **2021**, *268*, 113931. [CrossRef]
3. Patel, D.; Shrivastava, R.; Tiwari, R.P.; Yadav, R.K. Properties of cement mortar in substitution with waste fine glass powder and environmental impact study. *J. Build. Eng.* **2020**, *27*, 100940. [CrossRef]
4. Natali, A.; Manzi, S.; Bignozzi, M.C. Novel fiber-reinforced composite materials based on sustainable geopolymer matrix. In Proceedings of the International Conference on Green Buildings and Sustainable Cities, Bologna, Italy, 15–16 September 2011.
5. Garces, J.I.T.; Tan, R.R.; Beltran, A.B.; Ongpeng, J.M.C.; Promentilla, M.A.B. Environmental Life Cycle Assessment of Alkali-activated Material with Different Mix Designs and Self-healing Agents. *Chem. Eng. Trans.* **2021**, *88*, 835–840.
6. Ongpeng, J.M.C.; Guades, E.J.; Promentilla, M.A.B. CrossOrganizational Learning Approach in the Sustainable Use of Fly Ash for Geopolymer in the Philippine Construction Industry. *Sustainability* **2021**, *13*, 2454. [CrossRef]
7. Davidovits, J.; Comrie, D.C.; Paterson, J.H.; Ritcey, D.J. Geopolymeric Concretes for Environmental Protection. *ACI Concr. Int.* **1990**, *12*, 30–40.
8. Yoo, D.-Y.; Shin, H.-O.; Yang, J.-M.; Yoon, Y.-S. Material and bond properties of ultra high performance fiber reinforced concrete with micro steel fibers. *Compos. Part B Eng.* **2014**, *58*, 122–133. [CrossRef]
9. Liu, Y.; Zhang, Z.; Shi, C.; Zhu, D.; Li, N.; Deng, Y. Development of ultra-high performance geopolymer concrete (UHPGC): Influence of steel fiber on mechanical properties. *Cem. Concr. Compos.* **2020**, *112*, 103670. [CrossRef]
10. Berrocal, C.G.; Lundgren, K.; Löfgren, I. Influence of steel fibres on corrosion of reinforcement in concrete in chloride environments: A review. In Proceedings of the 7th International Conference Fibre Concrete, Prague, Czech Republic, 12–13 September 2013.

11. Lobregas, M.O.; Buniao, E.V.; Leaño, J.L. Alkali-enzymatic treatment of Bambusa blumeana textile fibers for natural fiber-based textile material production. *Ind. Crops Prod.* **2023**, *194*, 116268. [CrossRef]
12. Camargo, M.M.; Taye, E.A.; Roether, J.A.; Redda, D.T.; Boccaccini, A.R. A Review on Natural Fiber-Reinforced Geopolymer and Cement-Based Composites. *Materials* **2020**, *13*, 4603. [CrossRef]
13. Pilien, V.P.; Garciano, L.E.; Promentilla, M.A.; Guades, E.; Leaño, J., Jr.; Oreta, A.W.; Ongpeng, J.M. Fly ash Based Banana Fiber-reinforced Geopolymer Mortar. In *IABSE Symposium Prague 2022: Challenges for Existing and Oncoming Structures*; International Association for Bridge and Structural Engineering: Prague, Czech Republic, 2022; pp. 1212–1219.
14. Muthu, S.S. Introduction to sustainability and the textile supply chain and its environmental impact. In *Assessing the Environmental Impact of Textiles and the Clothing Supply Chain*; Woodhead Publishing: Cambridge, UK, 2020; pp. 1–32. [CrossRef]
15. Mejía Osorio, J.C.; Rodríguez Baracaldo, R.; Olaya Florez, J.J. The influence of alkali treatment on banana fibre's mechanical properties. *Ing. Investig.* **2012**, *32*, 83–87. [CrossRef]
16. Sivaranjana, P.; Arumugaprabu, V. A brief review on mechanical and thermal properties of banana fiber based hybrid composites. *SN Appl. Sci.* **2021**, *3*, 176. [CrossRef]
17. Lotfi, A.; Li, H.; Dao, D.V.; Prusty, G. Natural Fiber–Reinforced Composites: A Review on Material, Manufacturing, and Machinability. *J. Thermoplast. Compos. Mater.* **2021**, *34*, 238–284. [CrossRef]
18. Bharathi, V.; Vinodhkumar, S.; Saravanan, M.M. Strength characteristics of banana and sisal fiber reinforced composites. *IOP Conf. Ser. Mater. Sci. Eng.* **2021**, *1055*, 012024. [CrossRef]
19. Zhang, W.; Wu, J.; Gao, L.; Zhang, B.; Jiang, J.; Hu, J. Recyclable, Reprocessable, Self-Adhered and Repairable Carbon Fiber Reinforced Polymers Using Full Biobased Matrices from Camphoric Acid and Epoxidized Soybean Oil. *Green Chem.* **2021**, *23*, 2763–2772. [CrossRef]
20. Faruk, O.; Bledzki, A.K.; Fink, H.-P.; Sain, M. Progress Report on Natural Fiber Reinforced Composites. *Macromol. Mater. Eng.* **2013**, *299*, 9–26. [CrossRef]
21. Motaleb, K.Z.M.A.; Ahad, A.; Laureckiene, G.; Milasius, R. Innovative Banana Fiber Nonwoven Reinforced Polymer Composites: Pre- and Post-Treatment Effects on Physical and Mechanical Properties. *Polymers* **2021**, *13*, 3744. [CrossRef]
22. Koutas, L.N.; Tetta, Z.; Bournas, D.A.; Triantafillou, T.C. Strengthening of Concrete Structures with Textile Reinforced Mortars: State-of-the-Art Review. *J. Compos. Constr.* **2019**, *23*, 03118001. [CrossRef]
23. Banana Fibre Reinforced Cementatious Concrete. 2020. Available online: https://www.irejournals.com/paper-details/1701855 (accessed on 1 January 2023).
24. Ali, N.F.; Ali, S.H.; Ahmed, M.T.; Patel, S.K. Study on Strength Parameters of Concrete by adding Banana Fibers. *Int. Res. J. Eng. Technol.* **2020**, *7*, 3.
25. Mostafa, M.; Uddin, N. Effect of Banana Fibers on the Compressive and Flexural Strength of Compressed Earth Blocks. *Buildings* **2015**, *5*, 282–296. [CrossRef]
26. Wyom Paul, Z.; Abdul Shukor Lim, N.H.; Chau Khun, M. A scientometric review of geopolymer concrete. *J. Clean. Prod.* **2020**, *280*, 124353. [CrossRef]
27. Pilien, V.P.; Garciano, L.E.O.; Promentilla, M.A.B.; Guades, E.J.; Leaño, J.L., Jr.; Oreta, A.W.C.; Ongpeng, J.M.C. Optimization of Banana Fiber Reinforced Fly Ash Based Geopolymer Mortar. *Chem. Eng. Trans.* **2022**, *94*, 427–432.
28. Buller, A.S.; Abro, F.U.R.; Lee, K.-M.; Jang, S.Y. Mechanical Recovery of Cracked Fiber-Reinforced Mortar Incorporating Crystalline Admixture, Expansive Agent, and Geomaterial. *Adv. Mater. Sci. Eng.* **2019**, *2019*, 3420349. [CrossRef]
29. Mohamed, A.E.; Bernd, H. Combined effect of fine fly ash and packing density on the properties of high performance concrete: An experimental approach, Construct. *Build. Mater.* **2014**, *58*, 225–233.
30. Yoddumrong, P.; Rodsin, K.; Katawaethwarag, S. Seismic strengthening of low-strength RC concrete columns using low-cost glass fiber reinforced polymers (GFRPs). *Case Stud. Constr. Mater.* **2020**, *13*, e00383. [CrossRef]
31. Quiatchon, P.R.J.; Dollente, I.J.R.; Abulencia, A.B.; Libre, R.G.D.G., Jr.; Villoria, M.B.D.; Guades, E.J.; Promentilla, M.A.B.; Ongpeng, J.M.C. Investigation on the Compressive Strength and Time of Setting of Low-Calcium Fly Ash Geopolymer Paste Using Response Surface Methodology. *Polymers* **2021**, *13*, 3461. [CrossRef]
32. Cascardi, A.; Longo, F.; Micelli, F.; Aiello, M.A. Compression strength of confined columns with fiber reinforced mortar (FRM): New design-oriented models. *Constr. Build. Mater.* **2017**, *156*, 387–401. [CrossRef]
33. Leone, M.; Aiello, M.A.; Balsamo, A.; Carozzi, F.G.; Ceroni, F.; Corradi, M.; Gams, M.; Garbin, E.; Gattesco, N.; Krajewski, P.; et al. Glass fabric reinforced cementitious matrix: Tensile properties and bond performance on masonry substrate. *Compos. Part B Eng.* **2017**, *127*, 196–214. [CrossRef]
34. Kariou, F.A.; Triantafyllou, S.P.; Bournas, D.A.; Koutas, L.N. Out-of plane response of masonry walls strengthened using textile-mortar system. *Constr. Build. Mater.* **2018**, *165*, 769–781. [CrossRef]
35. Heng, K.; Areemit, N.; Chindaprasirt, P. Behavior of concrete cylinders confined by a ferro-geopolymer jacket in axial compression. *Eng. Appl. Sci. Res.* **2016**, *44*, 90–96. [CrossRef]
36. Tomoda, B.T.; Yassue-Cordeiro, P.H.; Ernesto, J.V.; Lopes, P.S.; Péres, L.O.; da Silva, C.F.; de Moraes, M.A. Characterization of biopolymer membranes and films: Physicochemical, mechanical, barrier, and biological properties. *Biopolym. Membr. Film.* **2020**, 67–95. [CrossRef]
37. Akinyemi, B.A.; Dai, C. Development of banana fibers and wood bottom ash modified cement mortars. *Constr. Build. Mater.* **2020**, *241*, 118041. [CrossRef]

38. Basu, P. (Ed.) Analytical Techniques. In *Biomass Gasification, Pyrolysis and Torrefaction*, 3rd ed.; Academic Press: Cambridge, MA, USA, 2018; Chapter 14; pp. 479–495. ISBN 9780128129920.
39. Holtzapple, M.T. Lignin. In *Encyclopedia of Food Sciences and Nutrition*, 2nd ed.; Caballero, B., Ed.; Academic Press: Cambridge, MA, USA, 2003; pp. 3535–3542. ISBN 9780122270550.
40. Mahir, F.; Keya, K.N.; Sarker, B.; Nahiun, K.; Khan, R. A brief review on natural fiber used as a replacement of synthetic fiber in polymer composites. *Mater. Eng. Res.* **2019**, *1*, 88–99. [CrossRef]
41. Zhang, P.; Han, X.; Hu, S.; Wang, J.; Wang, T. High-temperature behavior of polyvinyl alcohol fiber-reinforced metakaolin/fly ash-based geopolymer mortar. *Compos. Part B Eng.* **2022**, *244*, 110171. [CrossRef]
42. Oliveira, D.V.; Ghiassi, B.; Allahvirdizadeh, R.; Wang, X.; Mininno, G.; Silva, R.A. Macromodeling approach for pushover analysis of textile-reinforced mortar-strengthened masonry. In *Numerical Modeling of Masonry and Historical Structures*; Woodhead Publishing: Cambridge, UK, 2019; pp. 745–778.
43. De Felice, G.; De Santis, S.; Garmendia, L.; Ghiassi, B.; Larrinaga, P.; Lourenco, P.; Oliveira, D.; Paolacci, F.; Papanicolaou, C.G. Mortar-based systems for externally bonded strengthening of masonry. *Mater. Struct.* **2014**, *47*, 2021–2037. [CrossRef]
44. Naghizadeh, A.; Ekolu, S.O.; Musonda, I. High temperature heat—Treatment (HTHT) for partial mitigation of alkali attack in hardened fly ash geopolymer binders. *Case Stud. Constr. Mater.* **2020**, *12*, e00341. [CrossRef]
45. Riahi, S.; Nemati, A.; Khodabandeh, A.R.; Baghshahi, S. Investigation of interfacial and mechanical properties of alumina-coated steel fiber reinforced geopolymer composites. *Constr. Build. Mater.* **2021**, *288*, 123118. [CrossRef]
46. Snellings, R.; Mertens, G.; Elsen, J. Supplementary Cementitious Materials. *Rev. Mineral. Geochem.* **2012**, *74*, 211–278. [CrossRef]
47. Yun, H.-D.; Lee, J.-W.; Jang, Y.-I.; Jang, S.-J.; Choi, W. Microstructure and Mechanical Properties of Cement Mortar Containing Phase Change Materials. *Appl. Sci.* **2019**, *9*, 943. [CrossRef]